OPTIMISATION OF TURBOMACHINERY BLADE SHAPE USING 3D VISCOUS FLOW COMPUTATIONS

S.V. Yershov - A.V. Rusanov - V.A. Yakovlev

Aero Hydrodynamic Department,
Podgorny Institute for Mechanical Engineering Problems of National Academy of Sciences of Ukraine, Kharkov, Ukraine,
yershov@ipmach.kharkov.ua, rusanov@ipmach.kharkov.ua, yava@ipmach.kharkov.ua

ABSTRACT

Optimisation of 3D blade geometry for gas and steam turbines using 3D viscous flow computations is considered. The flow is described by the Reynolds averaged Navier-Stokes equations using the two-equation turbulence model. The equations are numerically integrated by a high-resolution scheme. The use of a state equation for calorically imperfect gas increases the accuracy of predicting steam flows. The problem statement accounts for the influence of film-cooling on the flow pattern and the turbine performance.

The input geometric variables determine the 3D shape of blades, including the compound lean, compound sweep, compound twist, etc. The objective function is turbine stage efficiency and the simplex method is used for its local maximum search.

The results of blade shape optimisation for different turbine stages are presented.

NOMENCLATURE

Symbols

a	blade throat
b	blade chord
D	mean diameter
f	objective function
F	fluxes
G	mass flow rate
H	source terms
I	enthalpy
J	Jacobian of co-ordinate transformation
k	turbulent kinetic energy
l	blade length
N	number of variable parameters
M	turbine stage torque
p	pressure
q	heat flux
Q	conservative variables
r	distance to rotation axis
s	blade pitch
t	time
T	temperature
u_j	Cartesian velocity components
U^i	contravariant velocity components
x_j	Cartesian co-ordinates x, y, z with origin at the axis of rotation
y_n	variable parameter
γ	specific heat ratio
δ	blade shape deviation from prototype
δ_{ij}	Kronecker's delta
λ	heat conductivity
μ	dynamic viscosity
ρ	density or stage reaction
τ_{ij}	tensor of viscous stresses
η	adiabatic efficiency
Ω	rotation speed
ψ^i	curvilinear co-ordinates ξ,η,ζ
$\overline{\psi}^i_j$	metric coefficients

Indices

*	total value
E, I	stage exit or inlet
i,j,k,l	integer upper and lower indices corresponding to curvilinear and Cartesian co-ordinates respectively
is	isentropic value
m	subiteration number or molecular
n	time step number or vertex number
t	turbulent

Abbreviations

BDF	backward difference formula
ENO	essentially non-oscillatory
RANS	Reynolds-averaged Navier-Stokes equations
SST	shear stress transport

INTRODUCTION

The problem of increasing turbine efficiency is extremely relevant for turbomachinery design. The classical approach of turbine blade design and optimisation is based on the 1D, 2D and quasi-3D flow models (Meazu, 1989, Cravero and Dawes, 1997, Shelton et al., 1993, Burguburu et al., 2003, and others). In these cases, the problem of achieving high efficiency is reduced to minimising various kinds of kinetic energy losses, such as profile losses, secondary losses, etc.

3D phenomena have a dramatic impact on kinetic energy losses and efficiency of turbomachinery. Therefore, 3D flow analyses are more accurate than 2D ones and the turbine flowpath optimisation problem based on advanced 3D flow computations is drawing ever more attention (Demeulenaere and Van Den Braembussche, 1998, Kämmerer et al., 2003, Lapworth and Shahpar, 2004, etc.). Using such approaches, one can design turbine stages with blades having a complex 3D geometry. Compound lean, compound sweep and compound twist blades obtained by optimisation have shown enhanced aerodynamic performance. The key point is that the approach suggested does not require separate consideration of profile losses, secondary losses and others for each blade row. In this case it suffices to search for a 3D blade geometry that ensures overall reduction of kinetic energy losses in a turbine flowpath.

The promising approach suggested by Pierret and Van Den Braembussche, 1998, is a combination of evolutionary methods in searching for a global extremum (such as the genetic algorithm) with an artificial neural network. The latter is used as a powerful prediction system for speeding up the optimisation process. The approach is applicable for design of high performance modern turbines, even without having a prototype. Nevertheless, the use of conventional optimisation methods, such as the simplex method, can be effective. In this paper, the authors demonstrate how this approach can improve the gas and steam turbine stages aerodynamically.

Various phenomena such as radial gap leakage, extraction and injection of working medium, film-cooling, etc, occur in turbine flowpaths with a substantial impact on turbine performance and main flow behaviour. These factors are usually not accounted for when optimising the turbine blading so the authors of the paper supply to this lack.

STATEMENT OF THE PROBLEM IN OPTIMISATION OF 3D BLADE GEOMETRY

We consider the following statement of the problem in optimisation of 3D blade geometry of turbine stage blading: it is necessary to find a local maximum of stage efficiency under constraints imposed on the flow conditions and variable geometric parameters. Blade geometry is modified by varying the following quantities for each blade plane section (by which the blade is designed): root stagger angle, shift in the section plane, blade-section camber, blade thickness, etc. Blade geometry is changed by deviation from the base configuration (prototype). To reduce the number of variable design parameters, the deviations are assumed either constant over the blade span or governed by the linear or piece-wise quadratic law. Definitions of some geometric parameters are given in the Appendix.

To secure global flow conditions, a constraint is imposed on the mass flow rate. If required, other aerodynamic parameters, such as the stage reaction and the absolute flow angle at the stage exit can be fixed additionally. The variation range is also defined for each variable parameter. The optimisation problem is solved by the simplex (deformed polyhedron) method proposed by Nelder and Mead, 1965. In addition, we can use other search methods, viz. the method developed by Torczon, 1989, and the genetic algorithm (Goldberg, 1989).

We apply an automatic script for successively running program modules, that execute the following operations in an endless loop:

– the optimisation method step and determination of variable geometric parameters for a new vertex of the simplex;

– generation of 3D geometry of the overall turbine flowpath (a new configuration);
– aerodynamic computation of the new configuration;
– processing the results of aerodynamic computation, and calculation of the objective function and output parameters for the new configuration; and
– a convergence check at the end of the iteration and loop exit if the optimisation process is convergent.

The statement of optimisation problem is described in detail by Yershov et al, 2001, Lampart and Yershov, 2003.

THE METHOD OF 3D VISCOUS FLOW SIMULATION

The 3D viscous compressible flow is simulated with a set of unsteady RANS equations written in a locally curvilinear body-fitted co-ordinate system, rotating with a constant angular speed Ω:

$$\frac{\partial Q}{\partial t}+\frac{\partial F^i}{\partial \psi_i}=H\,, \tag{1}$$

where

$$Q=J\begin{pmatrix}\rho\\ \rho u_1\\ \rho u_2\\ \rho u_3\\ h\end{pmatrix};\qquad F^i=J\begin{pmatrix}\rho U^i\\ \rho u_1 U^i+p\overline{\psi}_1^i-\tau_{1k}\overline{\psi}_k^i\\ \rho u_2 U^i+p\overline{\psi}_2^i-\tau_{2k}\overline{\psi}_k^i\\ \rho u_3 U^i+p\overline{\psi}_3^i-\tau_{3k}\overline{\psi}_k^i\\ (h+p)U^i-(u_l\tau_{kl}-q_k)\overline{\psi}_k^i\end{pmatrix};\qquad H=J\begin{pmatrix}0\\ 2\rho u_2\Omega+\rho\Omega^2 x_1\\ -2\rho u_1\Omega+\rho\Omega^2 x_2\\ 0\\ 0\end{pmatrix};$$

$$h=p/(\gamma-1)+\rho\left(u_l u_l-\Omega^2 r^2\right)/2+\rho k\;;\quad U^i=u_l\overline{\psi}_l^i\;;\quad \overline{\psi}_j^i=\partial\psi^i/\partial x_j\;;\quad q_k=-\lambda\partial T/\partial x_k\;;\quad \lambda=\lambda_m+\lambda_t\;;$$

$$\tau_{jk}=2\mu\left(S_{jk}-S_{ll}\delta_{jk}/3\right)-2\rho k\delta_{jk}/3;\;\mu=\mu_m+\mu_t\;;\;S_{jk}=0.5\left(\partial u_j/\partial x_k+\partial u_k/\partial x_j\right).$$

Here and below, the Einstein summation over repeated indices is used.

The statistic influence of turbulence on the mean flow is simulated by the SST two-equation turbulence model developed by Menter, 1994.

The governing equations are numerically integrated with the Godunov-type high-resolution scheme of second order accuracy suggested by Yershov, 1994. Convergence acceleration is achieved with the following iterative operator:

$$\left[\mathbf{I}+\frac{2}{3}\frac{\Delta t}{J}\frac{\partial}{\partial\psi_i^-}\mathbf{A}_i^+ +\frac{2}{3}\frac{\Delta t}{J}\frac{\partial}{\partial\psi_i^+}\mathbf{A}_i^- -\frac{2}{3}\Delta t\mathbf{B}\right]\delta Q^{n+1,m+1}= -\frac{2}{3}\Gamma\left[\frac{3\Delta Q^{n+1,m}-\Delta Q^n}{2}+\frac{\Delta t}{J}\frac{\partial {F^i}^{n+1,m}}{\partial\psi_i}-\Delta t{H}^{n+1,m}\right], \tag{2}$$

where

$$\mathbf{A}_i^{\pm}=\frac{\mathbf{A}_i\pm|\mathbf{A}_i|}{2}\;;\;\mathbf{A}_i=\frac{\partial F^i}{\partial Q}\;;\;\mathbf{B}=\frac{\partial H}{\partial Q}\;;\;\delta Q^{n+1,m+1}=Q^{n+1,m+1}-Q^{n+1,m}\;;\;\Delta Q^{n+1,m}=Q^{n+1,m}-Q^n$$

The square brackets in the right-hand side of equation (2) contain a fully implicit non-factored and non-linearised difference analogue of equation (1) obtained with BDF, whereas the operator included in the left-hand side of equation (2) can be linearised and factored approximately. The flux

derivatives in the right-hand side of equation (2) are approximated with finite volume techniques using exact Riemann solver and ENO reconstruction.

The scheme demonstrates high computational efficiency and robustness under off-design flow conditions and for coarse computational grids, which is critical for solving optimisation problems. The statement of the 3D flow problem and the numerical approach are described in detail by Yershov and Rusanov, 2001, Yershov et al., 2001, Lampart et al., 2001, and Lampart et al., 2005.

The results of flow computations are used for determining stage performance. The adiabatic efficiency of turbine stages (the objective function) is calculated as follows:

$$\eta = \frac{M\Omega}{G_{\mathrm{I}}\left(I_{\mathrm{I}}^{*} - I_{\mathrm{E}is}\right)}.$$

The mass flow rate, the stage reaction, and the absolute flow angle at the stage exit, which are defined by 3D flow computation, can be used for implementation of optimisation constraints.

NUMERICAL EXAMPLES OF STAGE OPTIMISATION

Several steam and gas turbines were optimised using the described technique. In all cases, the stage efficiency increased. Comparisons of the flow through the initial and improved stages have shown that the efficiency can be increased best by eliminating separation and/or reducing exit velocity losses. Herein the flow conditions have been retained and the mass flow rate change through the initial and optimised stages does not exceed 0.5 per cent.

We consider a base non-optimised turbine stage as the initial configuration (the initial vertex of the simplex). We create an initial simplex using a random number generator to determine the remaining N vertices. Here the condition of non-degeneracy is imposed. An optimisation process is considered convergent if the mean-square deviation of an objective function and variable parameters in the simplex vertices is less than certain prescribed quantities:

$$\sqrt{\frac{1}{N+1}\sum_{n=1}^{N+1}\left[f\left(y_n\right)-\bar{f}\right]^2} < \varepsilon_1; \quad \sqrt{\frac{1}{N+1}\sum_{n=1}^{N+1}\left(y_n-\bar{y}\right)^2} < \varepsilon_2; \quad \bar{f} = \frac{1}{N+1}\sum_{n=1}^{N+1} f\left(y_n\right); \quad \bar{y} = \frac{1}{N+1}\sum_{n=1}^{N+1} y_n \ .$$

For each case of optimisation, the convergence errors ε_1 and ε_2 are specified individually.

During optimisation, we used a coarse grid of roughly 75,000 cells per blade row for 3D viscous flow computations. Processor time for flow computation with such grid is no more than 1 hour for PC Intel Pentium 4 3.2 GHz. The verifying computations of the flow through the initial and improved stages require a grid with roughly 600,000 cells per blade row.

Optimisation of the gas turbine transonic stage

Table 1 summarises the geometric and gasdynamic data for the gas turbine stage under consideration.

Optimisation was performed with six variable design parameters, namely: sweep and lean angles of stator blade; root stagger angles of stator and rotor blades, and twist angles of stator and rotor blades. The constraint imposed on the mass flow rate was for its value to be nearly constant.

The optimisation process converged with a preset accuracy after 72 iterations (135 flow computations), requiring roughly 120 hours of CPU time for PC Intel Pentium 4 3.2 GHz.

Fig. 1 shows the Mach number contours for the initial and improved stages at the case section of the rotor. For initial design, as evident from Fig. 1a, flow separation occurs at the suction side of the blade behind the shock wave. Separation is eliminated for the optimised stage as seen in Figs. 1b and 2, which show the entropy contours at the cross-section behind the rotor. Calculations show that the adiabatic efficiency of the improved stage exceeds that of the initial one by 0.7 per cent.

Quantity		Initial		Optimised	
		Stator	Rotor	Stator	Rotor
Variable parameters	Root stagger angle, degree	57	30	57.4	29.5
	Twist angle, degree	0	21	0.4	19.9
	Sweep angle, degree	0	–	4.1	–
	Lean angle, degree	0	–	3.3	–
Fixed parameters	Relative blade length[1], l/b	0.403	0.802	0.403	0.802
	Relative blade pitch, s/b	0.729	0.885	0.729	0.885
	Blade fanning, D/l	10.90	9.89	10.90	9.89
	Blade number, z	19	34	19	34
	Stage pressure drop, p^*_1/p_E, , Pa	3.12		3.12	
Output parameters	Effective exit angle, $\alpha_{ef} = \sin^{-1}(a/s)$, degree	17.37	25.29	17.31	25.36
	Stage reaction, ρ	0.4066		0.3337	
Constraint	Mass flow rate, G_I, kg/s	1.762		1.754	
Objective	Adiabatic efficiency, η	0.8462		0.8531	

Table 1: Geometric and gasdynamic data of the gas turbine transonic stage

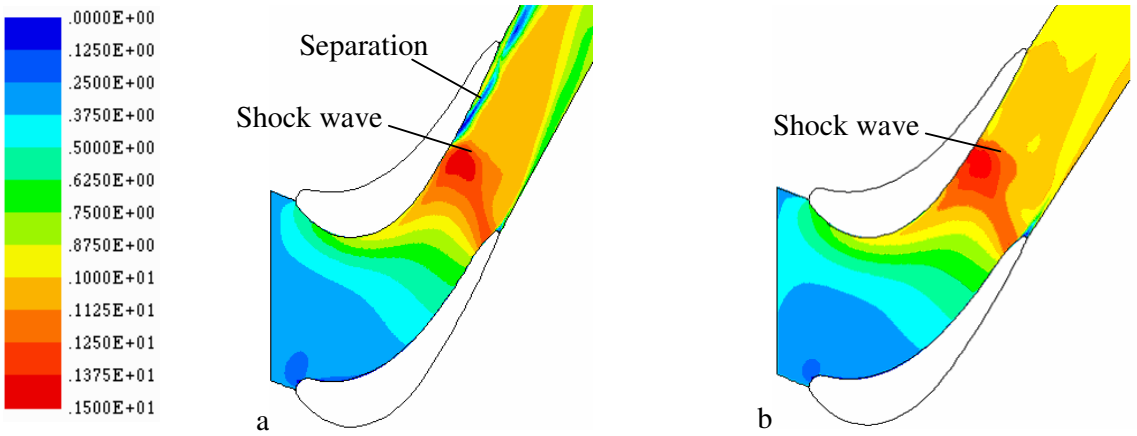

Fig. 1: Mach number contours at the rotor midspan for the initial (a) and optimised (b) stages

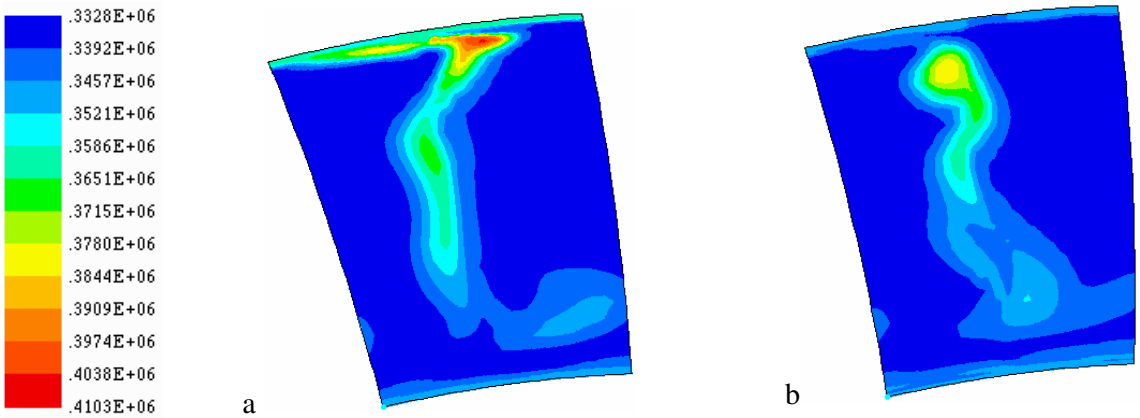

Fig. 2: Entropy function p/ρ^{γ} contours at cross-section behind the rotor for the initial (a) and optimised (b) stages

[1] Here and below the span-varying quantities are given for the mid-span blade section

Optimisation of the gas turbine subsonic stage

Fig. 3a demonstrates the initial shape of the low-pressure gas turbine subsonic stage. A distinctive feature of the stage is intensive film cooling that was taken into account during optimisation. Fig. 4 is the outline scheme of cooling air injection. The geometric and gasdynamic data of the stage are presented in Table 2.

Quantity		Initial		Optimised	
		Stator	Rotor	Stator	Rotor
Variable parameters	Root stagger angle , degree	-42.8	18.5	-37.0	21.2
	Twist angle, degree	-3.5	18.5	-16.7	20.3
	Lean angle, degree	0	-	0.9	-
Fixed parameters	Relative blade length, *l/b*	0.95	2.59	0.95	2.59
	Relative blade pitch, *s/b*	0.69	0.79	0.69	0.79
	Blade fanning, *D/l*	10.5	8.4	10.5	8.4
	Blade number, *z*	45	86	45	86
	Stage pressure drop, p^*_1/p_E, , Pa	2.23		2.23	
Output parameters	Effective exit angle, $\alpha_{ef} = \sin^{-1}(a/s)$, degree	18.8	29.9	19.0	26.7
	Stage reaction, ρ	0.190		0.275	
Constraint	Mass flow rate, G_1, kg/s	81.1		81.1	
Objective	Adiabatic efficiency, η	0.815		0.836	

Table 2: Geometric and gasdynamic data for the low-pressure gas turbine subsonic stage

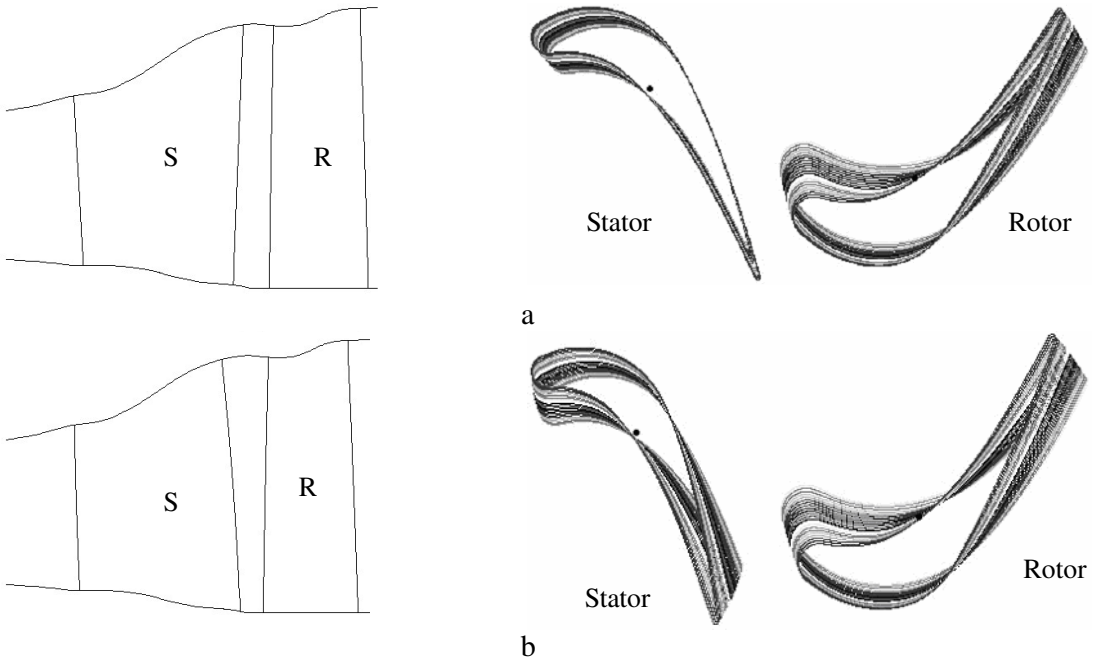

Fig.3: Initial (a) and optimised (b) geometry of the low-pressure gas turbine subsonic stage

Optimisation was performed with five variable parameters, viz. lean angle of stator; root stagger angles of stator and rotor, and twist angles of stator and rotor. The mass flow rate at the stage inlet was constrained to be a nearly constant value.

The optimisation process converged with preset accuracy after 105 iterations (183 flow computations), requiring roughly 160 hours of CPU time for PC Intel Pentium 4 3.2 GHz.

The optimised stage is shown in Fig. 3b. Optimisation yields increasing stage reaction near the blade root, where negative stage reaction was eliminated as evident in Fig. 5. In the issue, flow

separation at the suction side of the rotor blade near the root was removed (Fig. 6), with the adiabatic efficiency gain for the stage under consideration being about 2.1 per cent.

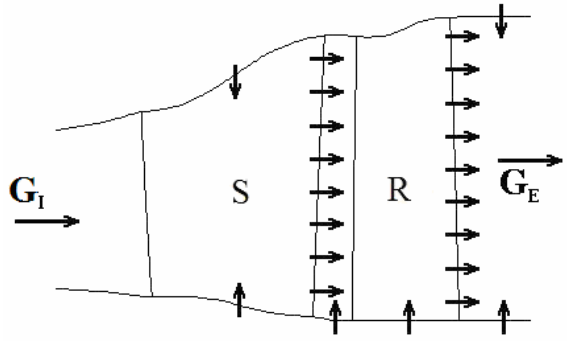

Fig.4: Outline scheme of cooling air injection for the low-pressure gas turbine subsonic stage

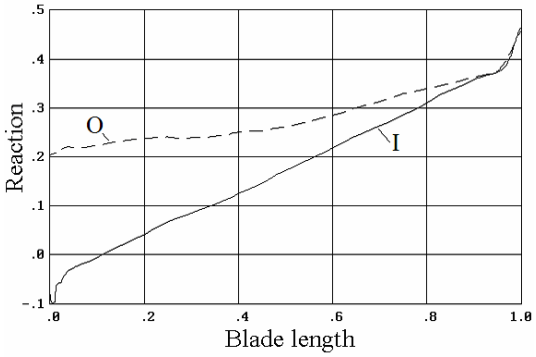

Fig.5: Distribution of low-pressure gas turbine subsonic stage reaction vs. blade length for initial (I) and optimised (O) design

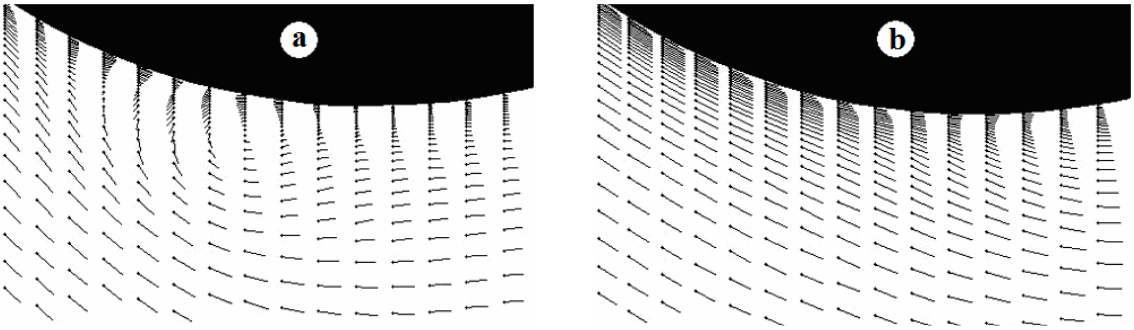

Fig.6: Velocity vectors near the rotor suction side of low-pressure gas turbine subsonic stage for initial (a) and optimised (b) design

Optimisation of the last stage of the steam turbine

We optimised the last stage of the low-pressure steam turbine. The initial shape of stage blades is shown in Fig. 7. The stator blade generatrices are straight lines for the initial stage. Table 3 summarises the geometric and gasdynamic data of the stage.

Quantity		Initial		Optimised	
		Stator	Rotor	Stator	Rotor
Variable parameters	Root stagger angle , degree	42.4	39.3	42.9	41.1
	Twist angle, degree	11	54.2	11	54.2
	Lean angle, degree	0	-	-6	-
	Compound lean and compound sweep	no	-	yes	-
Fixed parameters	Relative blade length, *l/b*	3.9	5.2	3.9	5.2
	Relative blade pitch, *s/b*	0.8	0.91	0.8	0.91
	Blade fanning, *D/l*	3.4	2.8	3.4	2.8
	Blade number, *z*	52	51	52	51
	Stage pressure drop, p^*_1/p_E, , Pa	2.93		2.93	
Output parameters	Effective exit angle, $\alpha_{ef} = \sin^{-1}(a/s)$, degree	18.4	26.8	18.4	25.3
	Stage reaction, ρ	0.2816		0.3495	
Constraint	Mass flow rate, G_I, kg/s	56.27		56.33	
Objective	Adiabatic efficiency, η	0.813		0.8246	

Table 3: Geometric and gasdynamic data of the last stage of the steam turbine

We varied seven geometric parameters, viz. the root stagger angles of the stator and rotor (at constant blade twists), the stator sweep angle, two parameters of stator compound sweep at the tip and two parameters of stator compound lean at the hub. The mass flow rate through the stage was constrained to be nearly constant. The leakage through the radial gap of the rotor row was account for during flow computations.

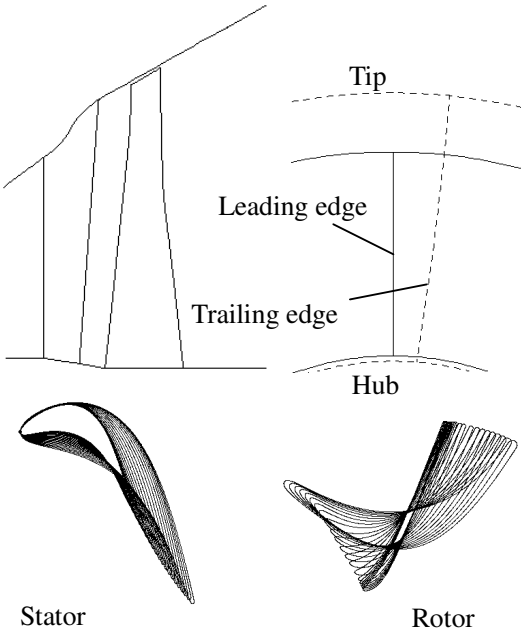

Fig. 7: Initial stage

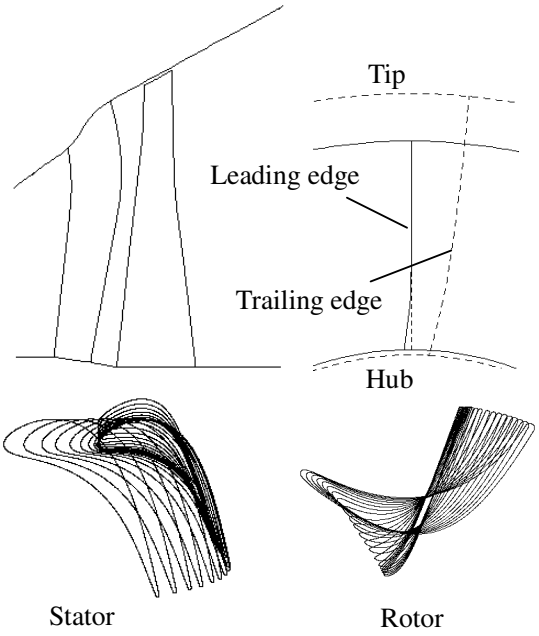

Fig. 8: Optimised stage

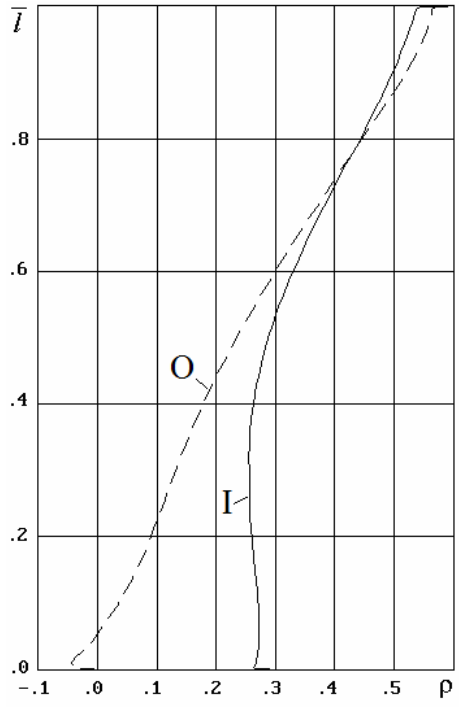

Fig. 9: Span distribution of stage reaction for initial (I) and optimised (O) design

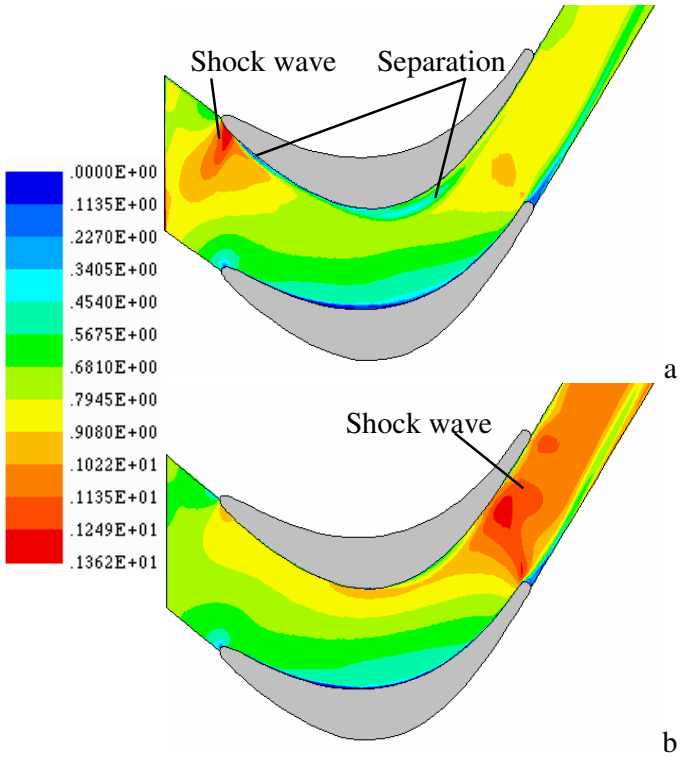

Fig. 10: Mach number contours at the root section of the rotor for initial (a) and optimised (b) stages

The optimisation process converged with a preset accuracy after 119 iterations (215 flow computations), requiring roughly 170 hours of CPU time for PC Intel Pentium 4 3.2 GHz.

Fig. 8 shows the shape of blades for the optimised stage with compound lean and sweep of the stator blade. The span distribution of stage reaction for initial and optimised stages is shown in Fig. 9. As evident, the negative reaction near root was eliminated due to optimisation and it favourably affects the flow in this region. Fig. 10 shows the Mach contours near the root section of the rotor for the initial and optimised stages. Evidently, the vane channel close to the hub became convergent and flow over-acceleration at the leading edge of the rotor blade near the root and the flow separation evoked thereby was eliminated as well. As a result, the adiabatic efficiency of the stage increased by almost 1.2 percent under design conditions.

The stage efficiency vs. mass flow rate dependence is shown in Fig. 11 for the initial stage (dashed line) and for the optimised one (solid line). The optimised stage is more efficient for design and especially for low-load conditions, where efficiency increase can exceed 10 percent. At the same time, for high-load conditions, the adiabatic efficiency of the initial stage is but little larger.

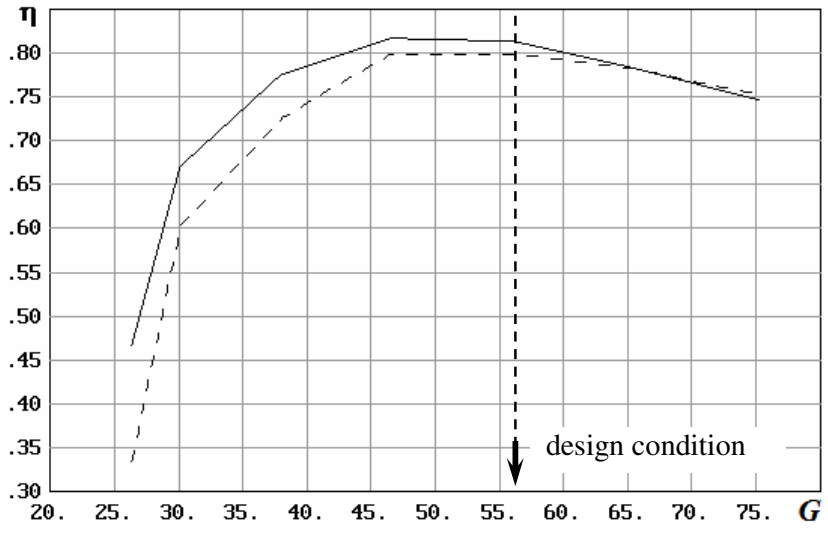

Fig. 11: Efficiency of stage vs. mass flow rate
— — — initial stage; ——— optimised stage

CONCLUSIONS

The potential of turbine flowpath optimisations is exploited by using the 3D viscous flow computation technique and the optimisation method of Nelder and Mead. Turbine performance was improved by optimising blade geometry using a compound lean, a compound sweep, and a twist of blades. For most cases of optimised stages, there was a pronounced increase in efficiency. The aerodynamic performance was improved mostly by eliminating flow separation.

Optimisation was carried out by coarse grid flow computations, whereas the performance of the initial and improved stages was compared finally on a refined grid. The numerical results obtained justify the feasibility of the approach suggested.

ACKNOWLEDGEMENTS

The authors express their sincere gratitude to Professors A. Gardzilewicz and A.L. Shubenko; Dr. P. Lampart; and designers and engineers B.V. Isakov, V.Ye. Spitsyn, M.A. Sharovskiy and A.A. Usatenko for many fruitful discussions.

REFERENCES

Burguburu, S., Toussaint, C., Bonhomme, C. and Leroy, G. (2003) *Numerical Optimization Of Turbomachinery Bladings*, Proceedings of ASME TurboExpo-2003, June 16–19, 2003, Atlanta, Atlanta, Georgia, USA, GT2003-38310, 11 p.

Cravero, C. and Dawes, W.N. (1997) *Throughflow Design using an Automatic Optimisation Strategy*, ASME Paper 97-GT-294, 12 p.

Demeulenaere, A. and Van Den Braembussche, R. (1998) *Three-dimensional inverse method for turbomachinery blading design*, ASME J. Turbomachinery, Vol. 120, No. 1, pp. 247–254.

Goldberg, D. (1989) Genetic Algorithms in Search, Optimization and Machine Learning, Addison-Wesley Publishing Corporation, 372 pp.

Kämmerer, S., Mayer, J.F., Paffrath, M., Wever, U. and Jung, A.R. (2003) *Three-Dimensional Optimization Of Turbomachinery Bladings Using Sensitivity Analysis*, Proceedings of ASME TurboExpo-2003, June 16–19, 2003, Atlanta, Atlanta, Georgia, USA, GT2003-38037, 9 p.

Lampart P., Gardzilewicz A., Yershov S., Rusanov A., (2001), *Investigation of interaction of the main flow with root and tip leakage flows in an axial turbine stage by means of a source/sink approach for a 3D Navier-Stokes Solver,* Journal of Thermal Science (JTS), International Journal of Thermal and Fluid Sciences, Vol. 10, No 3., pp. 198-204.

Lampart, P., Rusanov, A., Yershov, S., Marcinkowski, S. and Gardzilewicz, A. (2005) *Validation of a 3D RANS Solver With a State Equation of Thermally Perfect and Calorically Imperfect Gas on a Multi-Stage Low-Pressure Steam Turbine Flow*, Transactions of the ASME. Journal of Fluids Engineering, Vol. 127, No 1, pp. 83–93.

Lampart, P. and Yershov, S. (2003) *Direct Constrained Computational Fluid Dynamics Based Optimization of Three-Dimensional Blading for the Exit Stage of a Large Power Steam Turbine*, Transactions of ASME. J. Engineering for Gas Turbines and Power, Vol**.** 125, No. 1, pp. 385–390.

Lapworth, L. and Shahpar, S. (2004) *Design of gas turbine engines using CFD*, Proceedings of ECCOMAS 2004, Jyväskylä, July 24-28, 2004, pp. 1-21.

Meazu, G. (1989) *Blading Design for Axial Turbomachines, Overview on Blading Design Methods*, AGARD-LS-167, Propulsion and Energetics Panel.

Menter, F.R. (1994) *Two-equation eddy viscosity turbulence models for engineering applications*, AIAA J., Vol. 32, No. 11, pp. 1299–1310.

Nelder, J.A. and Mead, R. (1965) *A simplex method for function minimization*, The Computer Journal, Vol. 7, No. 1, pp. 308–313.

Pierret, S. and Van Den Braembussche, R., (1998) Turbomachinery blade design using a Navier-Stokes solver and artificial neural network. *ASME Paper* 1998-GT-4, 12 pp.

Shelton, M.L., Gregory, B.A., Lawson S.H., Moses H.L., Doughty, R.L. and Kiss, T. (1993) *Optimisation of a Transonic Turbine Airfoil Using Artificial Intelligence*, *CFD and Cascade Testing*, ASME Paper 93-GT-161, 14 pp.

Torczon, V.J. (1989) *Multi-Directional Search: A Direct Search Algorithm for Parallel Machines*, A Thesis Submitted in Partial Fulfillment of the Requirements f or the Degree Doctor of Philosophy Approved, Rice University, Houston, Texas, 114 p.

Yershov, S.V. (1994) *The Quasi-Monotonous ENO Scheme of Increased Accuracy for Integrating Euler and Navier-Stokes Equations*, Matematicheskoye Modelirovaniye (Mathematical Modelling), Vol. 6, No. 11, pp. 63–75 (in Russian).

Yershov S.V. and Rusanov A.V. (2001) *Numerical simulation of 3D viscous turbomachinery flow with high-resolution ENO scheme and modern turbulence model*, Task Quarterly, Vol. 5, No. 4, pp. 479–496.

Yershov, S.V., Rusanov, A.V. and Shapochka, A.Yu. (2001) *3D viscous transonic turbomachinery flows: numerical simulation and optimisation using code FlowER*, Internal Flows. Proc. of the Fifth Int. Symp.: Experimental and Computational Aerothermodynamics of Internal Flows, Sept. 4-7, 2001, Institute of Fluid-Flow Machinery of Polish Academy of Sciences, Gdansk, Poland, pp. 229-236.

APPENDIX: Definition of design variables

First, we consider design variables related to the stagger angles of blade sections. For each blade section, we specify the deviation of the stagger angle from that of the prototype, as shown in Fig. A1. Here the solid line is the prototype and the dashed line is a modified shape. If the deviation is constant along the blade span (line 1, Fig. A2), it corresponds to a turn of the blade as a whole through angle δ (design variable: "root stagger angle"). The linear span-wise distributed deviation shown in Fig. A2 by line 2 conforms to an additional blade twist (design variable: "blade twist"). The piece-wise parabolic distribution of stagger angle deviation near either one or both blade ends implements the nonlinear blade twist (design variables: "root compound twist", "tip compound twist", "root length", and "tip length").

The straight lean and the straight sweep of the blade are effected by turning the blade as a whole through certain angles in axial or/and circumferential directions.

The compound sweep and the compound lean of the blade can be implemented by shifts δ_1 and δ_2 of blade sections in their planes (see, Fig. A3) with a non-linear span-wise distribution similar to the compound twist as described above (Fig. A2).

Variation of the blade-section camber is effected by changing deviation δ, with a linearly axial-wise profile so as $S_1 = S_2 = S_3$ as shown in Fig. A4. Fig. A2 shows the possible span-wise distributions of this quantity.

Variation of blade thickness and maximum cross section location is implemented similarly.

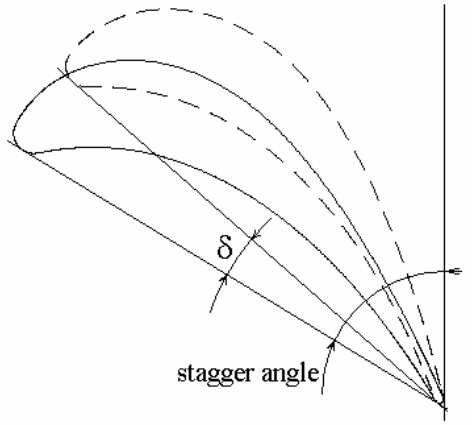

Fig. A1: Variation of stagger angle

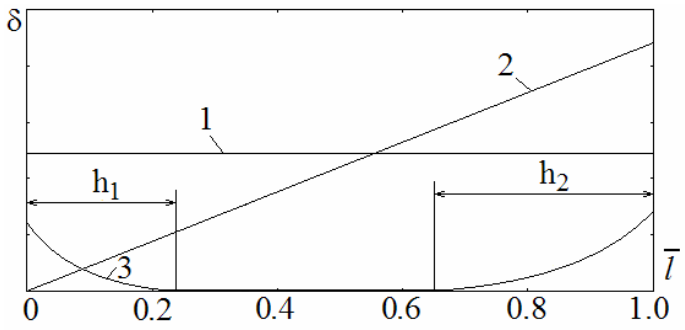

Fig. A2: Distribution of design variable δ along the blade span *l*

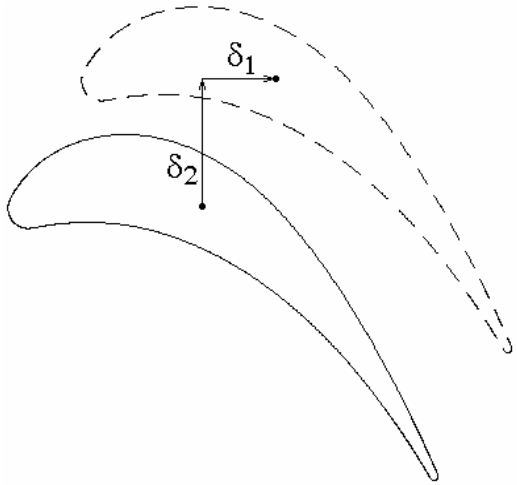

Fig. A3: Variation of plane section shift

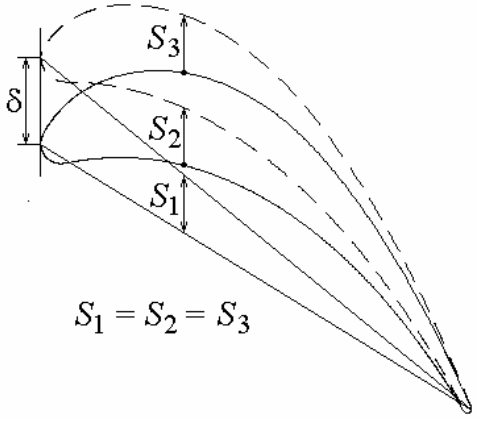

Fig. A4: Variation of blade-section camber